

## An Antarctic oceanographic section along 170°E\*

ARNOLD L. GORDON†

(Received 12 March 1974; in revised form 23 August 1974; accepted 21 September 1974)

**Abstract**—The circulation pattern of Antarctic and sub-Antarctic waters is strongly influenced by the complex marine topography south of New Zealand. The distribution of water characteristics indicates that the Antarctic Circumpolar Current undergoes intense wave-like migrations, which may be transient in nature, apparently associated with the Macquarie Ridge and Campbell Plateau. The bulk of the circumpolar current transport flows eastward over the northern flank of the mid-ocean ridge, but a strong, apparently jet-like, current exists around the periphery of the Campbell Plateau.

The water column of the upper 1000 m possesses much thermohaline complex structure on vertical scales of 20–200 m in the Polar Front zone along 170°E from 56 to 62°S. South of 62°S the water column is well stratified with a strong temperature minimum at 100 m, while north of 56°S is the well-mixed, thick, Sub-Antarctic Surface Water.

The geostrophic volume transport relative to the deepest common depth of station pairs, is  $135 \times 10^9 \text{ m}^3 \text{ s}^{-1}$ . The bottom velocities are not zero and the actual transport is quite different from the baroclinic transport. Bottom current (100 m above the sea floor) at 56°S average, for a three-day period, is  $29 \text{ cm s}^{-1}$  towards 065° T. Using this for geostrophic reference suggests that the current around the Campbell Plateau periphery has a surface zonal velocity of 1.5 knots.‡

### INTRODUCTION

ON APPROACHING the Macquarie Ridge the Antarctic Circumpolar Current (as revealed by the thermohaline distributions) shifts southward to follow the general trend of the mid-ocean ridge (DEACON, 1937). The interaction with the Macquarie Ridge appears to have a somewhat disruptive effect on the current structure (GORDON, 1972a) in that the flow divides into relatively narrow filaments at the two deep, narrow gaps in the ridge at 53°30'S and 56°S, with the bulk of the volume transport accomplished to the south of the Macquarie Ridge south of 58°S. Some of the flow apparently returns abruptly to the north by 'curling' around the southern tip of the Ridge into the Emerald Basin. The northern filaments continue to flow eastward to merge into a jet-like current ringing the southern and southeastern escarpments of the Campbell Plateau. It is not clear if the water derived from the southern tip of Macquarie Ridge joins this current or returns southward to join the apparent mainstream of the Circumpolar Current, which continues along the mid-ocean ridge about 800 km south of the Campbell Plateau.

The STD section along 170°E, obtained during *Eltanin* Cruise 50 in December, 1971, between 53 and 66°S (Fig. 1), allows more detailed discussion of the circulation south of New Zealand. The 170°E STD section is extended southward by *Eltanin* Cruises 27 and 32 STD stations into the southwestern Ross Sea, and northward of 53°S by *Eltanin* Cruise 36 STD data.

\*Lamont-Doherty Geological Observatory Contribution Number 2178.

†Lamont-Doherty Geological Observatory and Department of Geological Sciences, Columbia University, Palisades, New York 10964, U.S.A.

‡1 knot =  $0.51 \text{ m s}^{-1}$ .

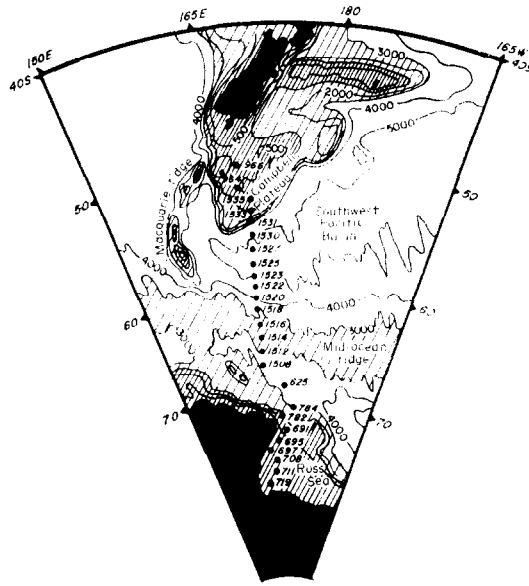


Fig. 1. Regional morphology and STD stations composing the 170°E section. Stations 1508–1535 are obtained from *Eltanin* Cruise 50 in December, 1971. The cruise 50 170°E profile is extended to the southwestern Ross Sea with STD data of *Eltanin* Cruises 27 and 32 (JACOBS and AMOS, 1967; JACOBS, BRUCHHAUSEN and BAUER, 1970) and to the north with *Eltanin* Cruise 36 STD station (JACOBS, BRUCHHAUSEN and BAUER, 1970). The bathymetry (contours in meters) is after HEEZEN, THARP and BENTLEY (1972). At the sites of Stas. 1514, 1523, and 1530, currents 100 m above the sea floor were also recorded.

## 2. THE DATA

The *Eltanin* Cruise 50 data were collected with the STD system of Plessey Environmental Systems (Model 9006) in conjunction with a surface-activated multiple sampler (SAMS) system (GERARD and AMOS, 1968), which is an array of Niskin bottles with reversing thermometers which are triggered from the ship, and provides standardization data for the STD output. The *Eltanin* systems are described in the data reports already cited and in JACOBS, BRUCHHAUSEN, ROSSELOT, GORDON, AMOS and BELLIARD (1972). The SAMS data are scattered throughout the water column, generally six levels for each down-trace of the STD. Some problems with the SAMS system were encountered during Cruise 50: the station pairs (a station pair is the STD down- and up-traces which are given separate station numbers since real variations are apparent in the comparison of the two traces) 1525–1526 and 1529–1530 have no SAMS data; neighboring stations are used for standardization. In the case of Sta. 1529 the salinity appears to be 0.01–0.02‰ too low, and it was decided to use 1530, the up-trace. All other stations in the profile are down-trace data. Another problem was encountered with Sta 1522: during descent the STD became inoperative at 2976 m. Below this depth two SAMS data points were obtained (3992 and 5012 m, the temperature change between these levels was only 0.04°C and the salinity change was 0.001‰).

Other data used in this report are near-bottom current meter measurements, mechanical bathythermograph (BT) and expendable bathythermography (XBT) observations, with surface salinity and silicate data, and compass-oriented bottom

photographs (described in the data reports of JACOBS, BRUCHHAUSEN, ROSSELOT, GORDON, AMOS and BELLIARD, 1972, and by THORNDIKE, 1959).

Three current-meter stations, obtained during Cruise 50, are used in this study. The method for current measurement used in recent *Eltanin* cruises can be briefly described: a Geodyne current-meter is positioned above the sea floor by two glass floats, which carry the system to the surface when a time-release mechanism detaches a set of weights.

### 3. TEMPERATURE, SALINITY AND WATER MASSES

The temperature and salinity are presented in three basic ways: the family of temperature versus depth and salinity versus depth traces from the STD records (Figs. 2a and 2b, respectively); a group temperature-salinity ( $T/S$ ) diagram of the standard-level data (Fig. 3); and profiles of the temperature and salinity fields projected on the 170°E meridional plane (Figs. 4 and 5, respectively). The temperature and salinity fields of the last two figures are extended to the southern Ross Sea and northward to the shallower portions of the Campbell Plateau to yield a useful picture of the thermohaline structure south and north of the Cruise 50 data.

There are five basic core layers, revealed by the 170°E data, within the water column, in addition to bottom water characteristics. These are listed in Table 1.

The salinity layer south of the mid-ocean ridge is not a circumpolar feature as are the other core layers (DEACON, 1937). Elsewhere the salinity decreases monotonically from the Circumpolar Deep Water (CDW) to the bottom, but near the Ross Sea the influence of the salty bottom water (GORDON, 1972b) produces such a deep  $S$ -min layer. The temperature maximum layer is indicated by the contrast of the cold surface layer with the warmer CDW; it can be considered as the upper boundary of the CDW. The salinity maximum results from the injection of saline deep water into the circumpolar belt in the Atlantic Ocean (REID and LYNN, 1971). The salinity of the CDW  $S$ -max decreases slowly on proceeding eastward, from a high of 34.90‰ at the introduction of the North Atlantic Deep Water, to a low of 34.73‰ in the Drake Passage (GORDON, 1971b).

#### A. Surface water

The upper kilometer of the water column along 170°E can be conveniently divided into three latitudinal zones: (1) an Antarctic zone, (2) a Polar Front zone, and (3) a Sub-Antarctic zone.

(1) *The Antarctic zone* is marked by horizontally lying isotherms and isohalines, fairly smooth temperature and salinity versus depth traces and a well-defined temperature minimum layer ( $T$ -min) near the base of relatively fresh Antarctic Surface Water (AASW). In winter the cold stratum of the  $T$ -min may extend to the sea surface at least in the southern regions of its distribution, and probably below the ice fields, but in summer, surface heating and additions of melt water isolate it from the sea surface and form the  $T$ -min layer (DEACON, 1933, 1937; MOSBY, 1934). In the northern range of its distribution it is observed most or all of the year and may be maintained by a northward flux (DEACON, 1937; GORDON, 1967) rather than produced *in situ* during the winter season.

The five southern STD stations of Cruise 50 represent the Antarctic **zone** in that they display a well-defined  $T$ -min layer (Fig. 2a), and the BT/XBT section in Fig. 8a

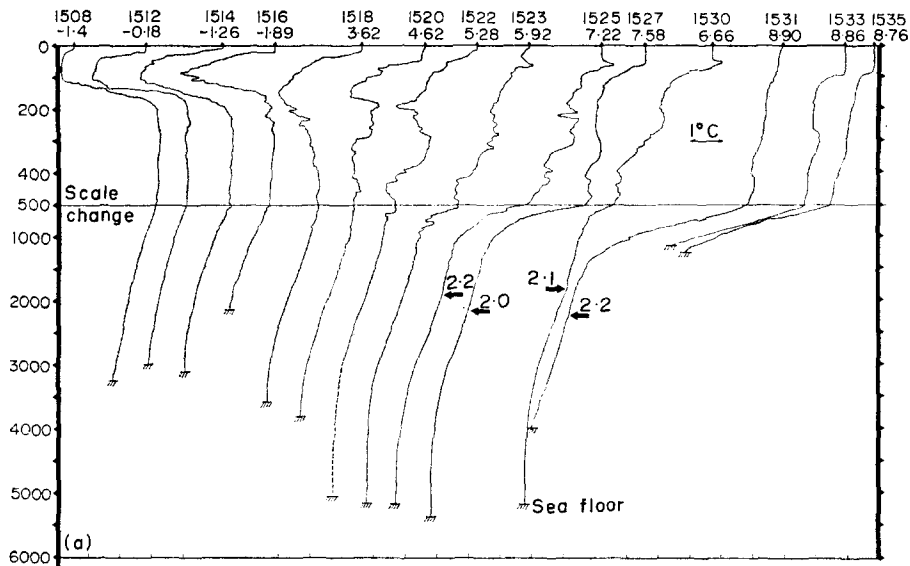
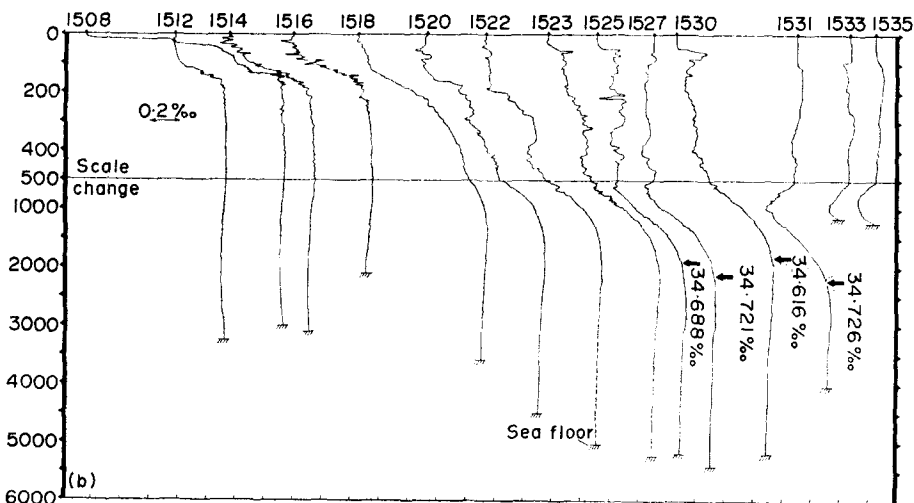


Fig. 2a. STD traces for temperature ( $^{\circ}\text{C}$ ) versus depth (m) for Cruise 50 data along  $170^{\circ}\text{E}$ .



b. STD trace for salinity ( $\text{‰}$ ) versus depth (m) for Cruise 50 data along  $170^{\circ}\text{E}$ . The Sta. 1522 traces are extended below 2933 m by water sample/reversing thermometer data near 4000 and 5000 m. The arrow with an associated temperature and salinity marks the position of the temperature gradient change ( $T$ -cusp), discussed in Section III-D.

indicates a predominant horizontal trend of the isotherms. This zone extends northward to  $62^{\circ}\text{S}$  (Sta. 1518). The two southernmost stations, 1508 and 1512, are colder, being less than  $0^{\circ}\text{C}$  at the surface and less than  $-1.8^{\circ}\text{C}$  within a  $T$ -min. A halocline occurs above the  $T$ -min layer resulting from melt-water additions to the immediate surface layer, and a weaker halocline occurs below the  $T$ -min which marks the transition to the CDW (Fig. 2b). The  $T$ -min layer itself is nearly homogeneous. The double nature of the halocline and broad  $T$ -min layer is found over a wide region south of Australia and New Zealand (GORDON, 1973).

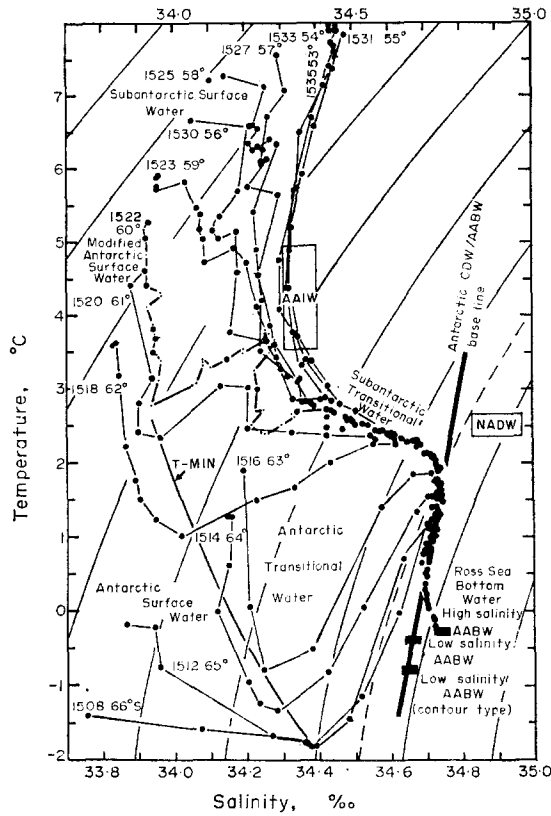


Fig. 3. Temperature/salinity plot of standard-level data for the Cruise 50 STD station along 170°E. Station 1522 *T/S* curve for the upper 500 m is constructed from STD data of 10-m intervals. Water-mass names are assigned according to the method given by GORDON (1971a, 1973). The *T/S* area marking the AAIW type is determined from all *Eltanin* data south of Australia and New Zealand. The North Atlantic Deep Water *T/S* area is taken for the South Atlantic (LYNN and REID, 1968; REID and LYNN, 1971). The modified Antarctic Surface Water results from summer heating of the near-surface water.

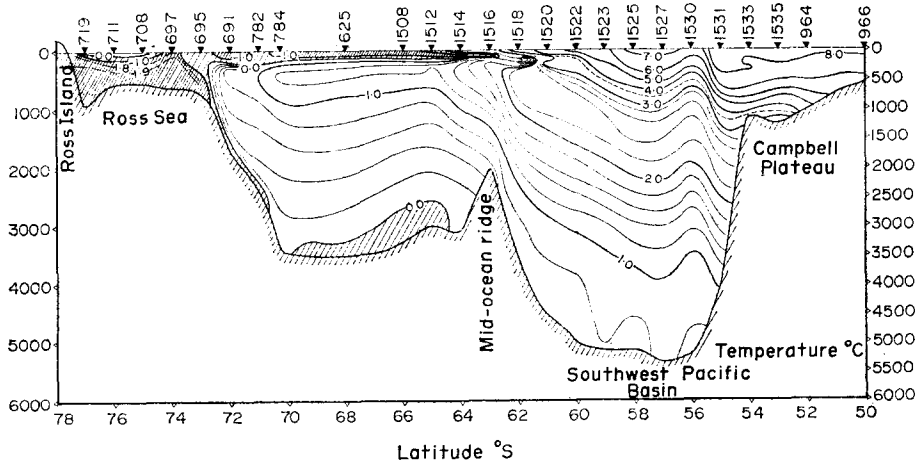


Fig. 4. Temperature (°C) field on the 170°E meridional plane constructed from data of the stations given in Fig. 1.

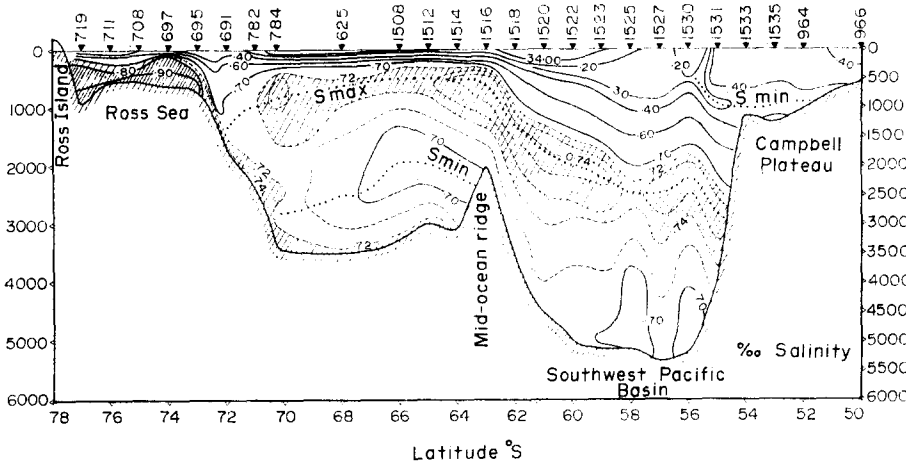


Fig. 5. Salinity (‰) field in the 170°E meridional plane constructed from data of the STD stations given in Fig. 1.

Table 1. Basic core layers along 170°E.

Core layer	Water mass	Ranges		
		T(°C)	S(‰)	Z(m)
Temperature minimum (south of polar front zone)	Antarctic Surface Water	-1.9-12.5	33.9-34.4	50-250
Temperature maximum (south of polar front zone)	Upper Circumpolar Deep Water	0.9-2.5	34.6-34.72	250-600
Salinity minimum (north of polar front zone)	Antarctic Intermediate Water	3.4-5.0	34.3-34.4	900
Deep salinity minimum (south of mid-ocean ridge)	Lower boundary of Circumpolar Deep Water	0.2-0.3	34.694-34.717	1900-2800
Salinity maximum	Lower Circumpolar Deep Water	1.0-1.8	34.704-34.748	500-3000
Bottom salinity maximum (south of mid-ocean ridge)	Ross Sea Bottom Water	-0.2-0.0	34.72-34.74	Bottom
Salinity maximum on continental shelf	Ross Sea Shelf Water	-2.2-1.8	34.8-34.97	Bottom

A characteristic temperature and salinity of the  $T$ -min layer in the southern two stations at 100 m depth is  $-1.83^{\circ}\text{C}$  and  $34.38\text{‰}$ . If these conditions extend to the sea surface in winter, then melting of 0.5 m and 0.4 m of sea ice is required to attain the observed salinity of Stas. 1508 and 1512, respectively.

Stations 1514 and 1516 reveal a warmer  $T$ -min layer:  $-1.34^{\circ}\text{C}$  at Sta. 1514 and  $-1.05^{\circ}\text{C}$  at 1516. The upper stratum is significantly warmer and saltier in comparison with the southern stations; however, the surface density difference from Stas. 1512 to 1514 is only 0.06 sigma- $t$  units.

(2) The *Polar Front zone* is observed north of Sta. 1518 ( $62^{\circ}\text{S}$ ) where  $T$ -min layer at 150 m is much warmer and fresher than is the case in the Antarctic zone. The  $T$ -min north of Sta. 1518 is comprised of an array of weak  $T$ -min layers rather than a

single well-defined layer. The BT/XBT profile along 170°E (Fig. 8), and at other meridians (GORDON, 1971c), indicate isotherms north of the well-stratified Antarctic water column zone have noticeable vertical trends and complex structure. Within the Polar Front zone lies the transition from Antarctic to Sub-Antarctic Surface Water, i.e. the Polar Front or (as some prefer) the Antarctic Convergence. Along 170°E the Polar Front is located in the central to southern parts of the Polar Front zone near 59°S; this latitude marks the northern limits of the *T*-min and of low surface salinity (less than 34‰) which are often taken as expressions of the Polar Front. However, it is more appropriate to consider a Polar Front zone rather than a single line of discontinuity (though in some areas at particular times the zone may be quite narrow and well marked).

The degree of structure with a scale of 20–200 m in vertical extent within the upper 500 m increases markedly at 61°S and continues to 56°S. The structures with lower temperature are associated with lower salinity, while the warm layers are saltier. Lateral eddies acting along density surfaces would be most effective in causing interleaving of water types when the larger scale (or climatic) thermohaline field possess sloping isopleths relative to the isosteres, as is the case for the region from 62 to 55°S (see STOMMEL and FEDOROV, 1967; and PINGREE, 1972). The trend of the isotherms and isohalines must have opposite slopes for lateral mixing to produce the relations of temperature to salinity in the observed structures. This occurs only between Stas. 1520 and 1531, i.e. 61–55°S, from the surface to 500 m (down to 250 m for Sta. 1520). South of Sta. 1518 the flat-lying isopleths are not favorable for generation of interleaving by lateral eddies.

(3) North of 56°S the surface layer becomes less complex. The upper 500 m are relatively isothermal and isohaline. Such a mixed region is typical of the southern section of the *Sub-Antarctic zone*, which generally extends to the Polar Front (DEACON, 1933, 1937), but in the case of the 170°E section it terminates 300–400 km north of the Polar Front. This 300–400-km intervening belt (56–59°S) is Sub-Antarctic Surface Water as revealed by the *T/S* diagram (Fig. 3), but it has more complex thermohaline structure than is more typically the case. The stations to the north of the Polar Front zone are separated from the Polar Front zone by a frontal structure which BURLING (1961) calls the Australasian Sub-Antarctic Front.

*Temperature-salinity relation of the surface layer.* The *T/S* curves constructed from the standard-level data (Fig. 3) show that the four southern stations within the Antarctic zone smoothly curve from the surface layer through the *T*-min stratum to the *T*-max of the upper CDW. Station 1518, which marks the southern limits of the complex zone, also shows a smooth trend, though at significantly higher temperature and lower salinity at the *T*-min layer. The *T*-min of Sta. 1518 is similar to the immediate surface waters of the south. The *T/S* curves of the stations within the Polar Front zone as expected show more structure. The interleaving of water types revealed by the 10-m data points for Sta. 1522 appear to parallel sigma-*t* lines as noted by GREGG and COX (1972). The fate of these structures is not known, nor is their importance to Antarctic Circumpolar Current dynamics and production of Antarctic Intermediate Water, both of which are associated with the Polar Front zone (WYRTKI, 1960).

#### B. Antarctic Intermediate Water (AAIW)

Stations 1531–1535, from 55 to 53°S, reveal a salinity minimum (*S*-min) at

approximately 900 m. The *S*-min layer is, for the most part, 200–300 m above the floor of the southern Campbell Plateau and reaches the bottom farther north. The *S*-min layer extends northward in each ocean below the main thermocline, and is known as the Antarctic Intermediate Water mass (AAIW).

Inspection of the group *T/S* diagram, Fig. 3, shows the three *S*-min points (Stas. 1531–1535) to fall close together. All *Eltanin* *S*-min data-points south of Australia and New Zealand (Cruises 36–49 about 60 points total) fall in the *T/S* area shown in Fig. 3. The range of temperature of the AAIW is 3.4 to 5.0°C, and of salinity 34.3–34.4‰; the average being 4.4°C and 34.36‰, which is near the average given by SVERDRUP (1940) (4.4°C and 34.39‰), based on many less points of the *Banzare* data of 1930 and 1931 (HOWARD, 1940). It is remarkable that the characteristics of AAIW appear to be as steady as indicated by comparison of DEACON's (1937), SVERDRUP's (1940), and WUST's (1935) core values and those observed by *Eltanin*.

The *T/S* curve passing through the *S*-min layer of the AAIW observed north of 55°S is similar in density (though slightly warmer and saltier) to the *T/S* points at the base of the nearly isohaline surface layers north of the Polar Front revealed by Stas. 1525–1530. The junction of the surface (isohaline) to deeper (isothermal) water north of the Polar Front occurs from 3.5 to 4.0°C and 34.2 to 34.3‰ and at depths of 500–700 m. It is apparent in the salinity section (Fig. 5) as an increased separation of the 34.2 and 34.3‰ isohalines; note, it is also observed as a warm-saline intrusion on the STD record of Sta. 1522, as the layer between 300 and 400 m.

With a northward component of flow this water type would pass between the warmer saltier mass of the Sub-Antarctic Surface Water and the colder, saltier transitional water mass (see Figs. 3–5), and on mixing with these waters could form the AAIW characteristics. The Sub-Antarctic Surface Water results from the action of local heating and influx from the north of subtropical waters (DEACON, 1937), and the transitional water is maintained by the upper CDW.

### C. Transitional water

The separation of the CDW from the fresher surface and intermediate waters occurs in a relatively stable transitional layer north of the Polar Front. The *T/S* characteristics of the transitional layer are nearly a straight line from the base of the surface's more isohaline water to the CDW/AABW curve (described below). Within and north of the Polar Front these curves intersect at nearly right angles and the transition water differs little from station to station. South of the front the transition waters vary greatly with distance from the front or with temperature of the near-surface *T*-min layer.

The transitional water is composed of a blend of surface and deep water. In each case, salt would diffuse upward, and south of the front; so would heat. A winter period process of increased vertical mixing may occur as the *T*-min layer becomes denser due to salt injection from ice formation. The *T/S* relation (Fig. 3) indicates a continuous increase of density of the *T*-min layer as latitude increases. In the southern two stations of the Cruise 50 data the *T*-min *T/S* points fall close to the density, which would allow convection or mixing with deep water when the non-linear character of the equation of state is taken into account (FOFONOFF, 1956; GORDON, 1971a), especially when greater compressibility of cold water is taken into account (GILL, 1973). Winter convection, below the ice, from the surface to the *T*-max level

would represent an effective process in upward flux of heat and salt within the Antarctic water column.

It is probable that within the transition layer a balance is achieved between the climatic (long-term average) upwelling due to surface layer Ekman divergence and turbulent deepening of Antarctic characteristics into the deep water. When these factors are in balance, the pycnocline or transitional water mass remains stationary in characteristics and depth, but local imbalance would result in shallowing or deepening of this layer.

The balance between upwelling in the transition layer and deepening by turbulence can be written as:

$$V \Delta S = A_z \frac{\Delta S}{\Delta Z} \quad ,$$

where  $V$  is the upwelling rate,  $A_z$  is the vertical mixing coefficient,  $\Delta S$  is the salinity difference across the transition zone, and  $\Delta Z$  is the thickness. The Ekman divergence of the surface water south of the Polar Front induces upwelling of  $54 \times 10^6 \text{ m}^3 \text{ s}^{-1}$  (GORDON, 1971a). Since not all of this water is necessarily deep water, but could be recirculating surface water, the average upwelling velocity of  $2.6 \times 10^{-4} \text{ cm s}^{-1}$  (derived by dividing by the area south of the Polar Front) represents an upper limit for the upwelling deep water. The  $\Delta S$  is approximately 0.6‰ and  $\Delta S/\Delta Z$  about  $4.0 \times 10^{-5}$ – $7.0 \times 10^{-5}$  for the northern and southern halves of the Antarctic Surface Water, respectively, a vertical mixing coefficient of  $4 \text{ cm}^2 \text{ s}^{-1}$  in the northern region, and  $2 \text{ cm}^2 \text{ s}^{-1}$  in the southern region, would be maximum values.

#### D. Deep water

(1) *Salinity and temperature maximum core layers.* On inspection of Antarctic group  $T/S$  diagrams given by GORDON (1971a, Figs. 4 and 5), and GORDON and GOLDBERG (1970, Figs. 3–5) it is apparent that below the  $S$ -max core layer of the CDW the  $T/S$  distribution is essentially linear. Along 170°E this relation is disturbed for water colder than 0.5°C by the introduction of the saline bottom water from the Ross Sea. A CDW/AABW baseline which parallels the middle of the linear section of the  $T/S$  scatter of the 170° data is added to Fig. 3. The linear nature of this baseline denotes an origin involving mixing of a bottom water type which is cold and relatively fresh and a deep water type which is warmer and saltier. The warm, saline influence is probably North Atlantic Deep Water (NADW) (LYNN and REID, 1968; REID and LYNN, 1971).

The extension of the CDW/AABW baseline, based on the 170°E data, to lower temperatures intersects the two low-salinity water types of Antarctic Bottom Water (Fig. 3). However, the extension of the base line to warmer temperatures does not intercept the  $T/S$  position of the NADW; it is somewhat lower in salinity than expected. In order to investigate this further, the CDW/AABW baseline which coincides with the data along 170°E is added to the temperature–salinity scatter of circumpolar points at the salinity maximum core layer (Fig. 6). The  $T/S$ -max data points in the eastern Pacific area fall to the low salinity side of the 170°E CDW/AABW baseline. The  $T/S$ -max data points in the southeast Atlantic, Indian and southwestern Pacific fall along the 170°E baseline. Therefore it is proposed that the relatively fresh southeast Pacific CDW, on passing into the Atlantic Ocean via the Drake Passage, mixes with the relatively saline NADW (approximately the same density) to form the

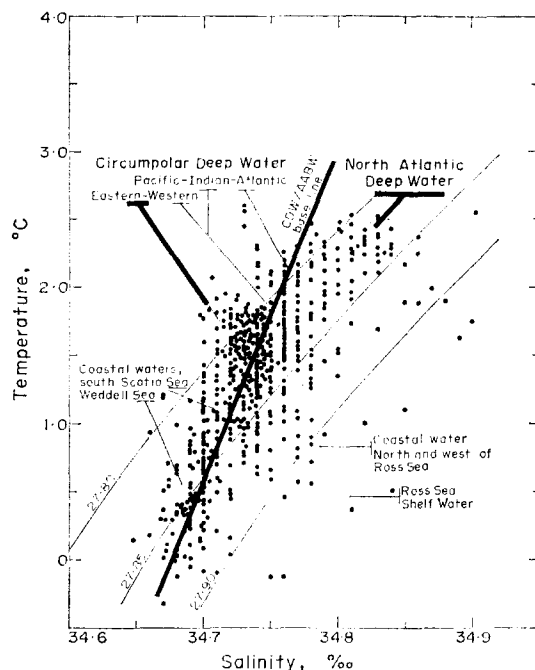


Fig. 6. Group temperature/salinity plot of points within the salinity-maximum layer ( $T$ - $S$  max) around Antarctica (taken from GORDON, 1971b) with the position of the  $170^{\circ}\text{E}$  CDW/AABW baseline.

CDW characteristic of the southeast Atlantic, Indian and southwest Pacific oceans. In the case of the southeast Atlantic, the  $T/S$ -max scatter (Fig. 6) suggest a 1 : 1 mixture of southeast Pacific CDW to NADW.

Why do  $T/S$ -max data points of the southeast Pacific fall to the left of the CDW/AABW baseline? There must be a low salinity water type besides AABW influencing the CDW characteristics within the Pacific Ocean. One immediately thinks of AAIW and/or the intermediate waters produced in the North Pacific (REID, 1965). BOLIN and STOMMEL (1961) and CRAIG and GORDON (1965) also note the influence of the North Pacific Intermediate Water and AAIW on 'common deep water' in that the salinity is lower than is expected from a simple mixture of NADW and AABW.

To the north of the Polar Front the  $T/S$  position of the  $S$ -max layer and of the transitional water mass layer does not vary much. However, in the case of the  $170^{\circ}\text{E}$  section, the temperature of the  $S$ -max layer begins to drop rapidly with increasing distance to the south of the Polar Front ( $62^{\circ}\text{S}$ ); this 'sliding' of the  $T/S$  max point down the CDW/AABW baseline apparently results from the increased downward penetration of the cold, low-salinity surface water south of the front into the shallowing depths of the deep water. In this sense, the  $S$ -max south of the Polar Front may be considered as an 'induced' core layer, since it is not a surface of spreading of a water mass, but rather the top of an 'undisturbed' water column segment.

The  $S$ -max of the Cruise 50 data along  $170^{\circ}\text{E}$  reaches a maximum of  $34.749\text{‰}$ . This is significantly below the maximum values of  $34.764\text{‰}$  in the southern Macquarie Ridge area and  $34.766\text{‰}$  at *Eltanin* Sta. 738 at  $63^{\circ}\text{S}$ ,  $178^{\circ}\text{E}$ .

Inspection of all *Eltanin*  $S$ -max data points south of New Zealand indicates a

patchy salinity distribution (Fig. 7). The depth of the *S*-max layer, however, is smooth to the extent that neighbouring stations fit quite easily into an isobath distribution. The salinity variations of the *S*-max core layer are associated with salinity variations of the *T/S* curve below the *S*-max point from the CDW/AABW baseline in such a way that the *T/S* curve remains nearly parallel to the baseline. These shifts are larger than measurement error and are considered to be real. The cause of this patchiness of the water column salinity below the *S*-max core layer is not known.

The *T*-max core layer of the upper portion of the CDW falls to the left (lower salinity) of the local CDW/AABW baseline. The *T*-max is the point on the *T/S* diagram where the lower temperature of the surface water begins to over-ride the warming effect of the upper layers of CDW. The salinity increase accompanying the *T*-max decrease on proceeding south of the Polar Front (Fig. 3) is an indication of differential motion of deep and surface layers; if both relatively warm-saline deep and cold-front surface water were to mix without differential motion, the *T*-max point would progressively move to cold and fresher values. Since this does not occur, the deep water apparently slides with a southward component below progressively colder surface water and mixes vertically with this water en route.

Between the *T*-max and *S*-max there is an Antarctic influence, since the *T/S* points of this stratum fall to the left of the CDW/AABW baseline. The source of this water may be from the south, where a convective interchange between the *T*-min and *T*-max 'feeds' relatively cold-fresh water into the density stratum occupying the region between the *T*-max and *S*-max further north.

(2) *Temperature cusp*. Immediately above the *S*-max core layer, near the 2°C isotherm, north of the Polar Front, is a sudden change in the slope of the temperature versus depth curve. This feature, temperature cusp, is observed on other STD records south of New Zealand and Australia for Cruise 36 of *Eltanin* (see *Eltanin* STD Stas. 938 and 940 of Cruise 36, JACOBS, BRUCHHAUSEN and BAUER, 1970), (see Table 2).

CRAIG, CHUNG and FIADEIRO (1972) discuss a similar feature in the southwest Pacific as a benthic thermocline and that it denotes differential moving water layers.

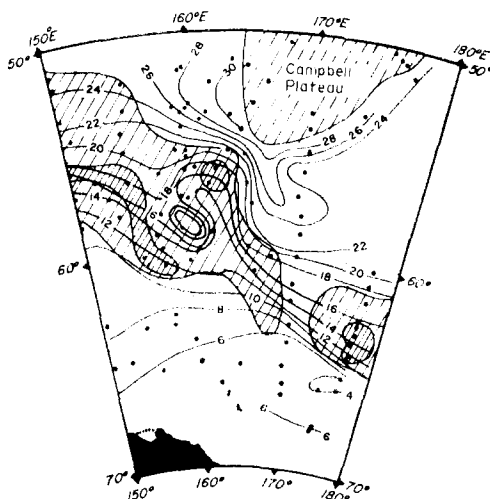


Fig. 7. Depth of the *S*-max layer south of New Zealand in hundreds of meters. Areas with salinity in excess of 34.75‰ are shown by the lighter line pattern and areas with salinity in excess of 34.76‰ are shown by the denser line pattern.

Table 2. Deep vertical temperature gradients at four Eltanin states for the 500-m interval above and below the temperature cusp.

Eltanin station	Average temperature gradient ( $10^{-5} \text{ }^{\circ}\text{C cm}^{-1}$ )		$\Delta$ in gradient ( $10^{-5} \text{ }^{\circ}\text{C cm}^{-1}$ )
	Above T-cusp	Below T-cusp	
938	0.64	0.94	+ 0.30
940	0.56	0.86	+ 0.30
1525	0.50	1.00	+ 0.50
1527	0.60	0.76	+ 0.16
Average increase			+ 0.315 $\times 10^{-5} \text{ }^{\circ}\text{C cm}^{-1}$

They note the existence of the Antarctic feature and they conclude that it is not related to the benthic thermocline, "... but is an advective feature associated with the salinity maximum, derived from the North Atlantic Deep Water". The investigation of the origin of the Antarctic *T*-cusp must await the availability of STD measurements in the Antarctic sectors of the South Atlantic and Indian oceans.

#### E. Bottom Water

The bottom water south of the mid-ocean ridge along 170°E is a high-salinity variety produced in the Ross Sea. The extension of the meridional sections to the Ross Sea reveals the thermohaline structure at a continental margin where bottom water is produced. The massive volume of near-freezing-point saline shelf water contributes to the saline water over the floor of the continental slope. The downward penetration of the near-surface isohalines over the slope region is similar to that discussed by GILL (1973).

#### 4. FRONTAL ZONES

Between the STD stations, BT and XBT observations were obtained at approximately 10-nautical-mile intervals.\* With the BT/XBT profiles, surface-water samples were collected for determination of surface salinity and silicate concentration. Since the AutoAnalyzer® was inoperative during the last third of Cruise 50, the surface silicate samples were stored in plastic bottles after adding chloroform for preservation. These samples were run at Lamont-Doherty in mid-February, 1972 (two months after collection). On proceeding northward along 170°E, a current meter (see Section 5) was set out at 59°S near Sta. 1523 for a three-day interval while the ship back-tracked to 63°S and returned to 59°S to obtain two more BT/XBT sections in that interval for time-variability study of the thermal structures.

The thermal structure of the upper few hundred meters between 53 and 65°S (Fig. 8a) is basically one of a well-defined *T*-min with mostly horizontally trending isotherms south of 62°S, which is the typical Antarctic zone. The surface temperature gradients are somewhat higher between about 62°30' and 63°S, and at 62°15'–62°28'S the change in surface salinity of nearly 0.30‰ is a well-marked feature (note this abrupt change is over the mid-ocean ridge). The sudden change in thermal structure and surface salinity (silicates are discussed below) between 62 and 62°30'S is repeated in Figs. 8b and c. This remarkable change in surface salinity and the deepening of the

\*1 nautical mile = 1.853 km.

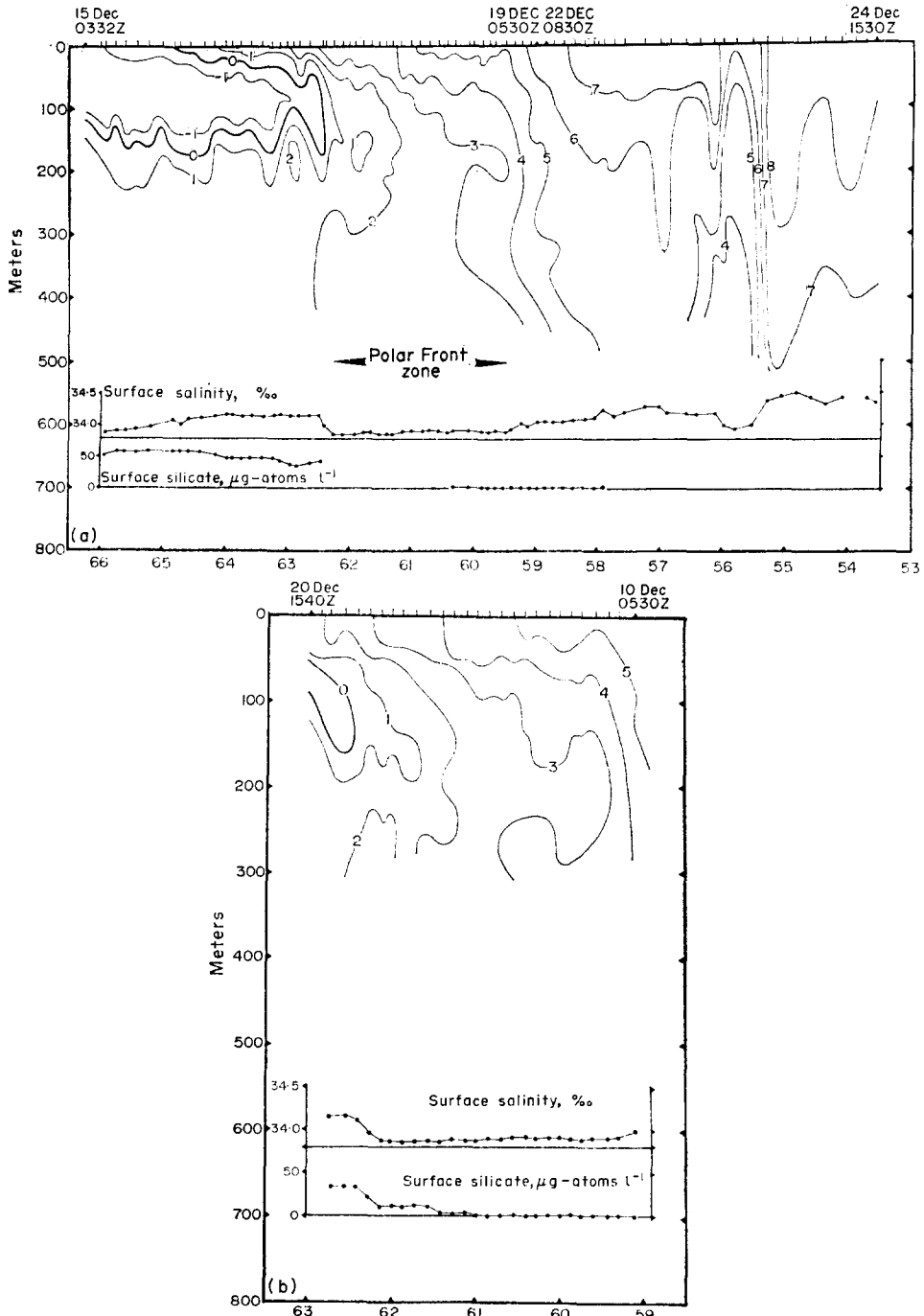
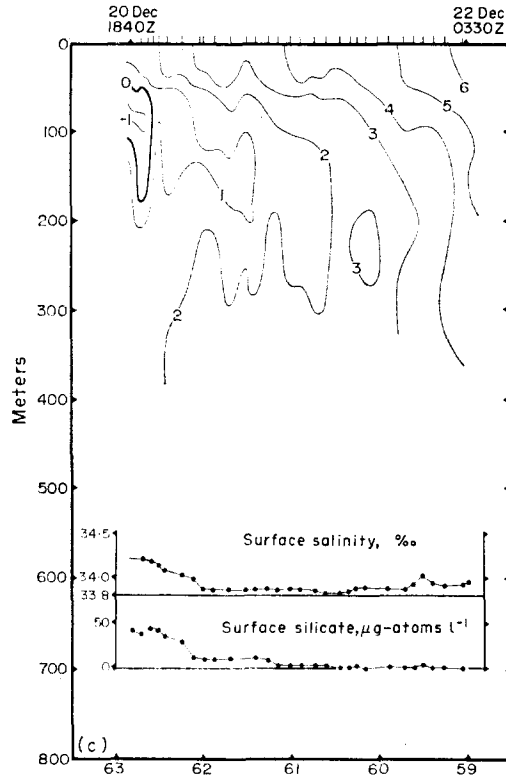


Fig. 8a. Thermal structure of the upper 500 m along 170°E from BT, XBT, and STD data obtained during Cruise 50. Surface salinity and silicate at nearly every BT/XBT and STD observation are given. The observations from the ice to 59°S (15–19, December, 1971) were taken while travelling northward and those north of 59°S (after 22 December, 1971) were obtained after a southward and return track to 63°S (Figs. 8b and 8c) along 170°E.  
 b. Thermal structure recorded by BT with surface salinity and silicate along 170°E (19–20 December 1971).



c. Thermal structure recorded by BT and XBT with surface salinity and silicate along 170°E (20–22 December, 1971).

*T*-min water to the north is a real discontinuity which separates differing characteristic water columns. It separates the thermally well-stratified Antarctic water column from the more complex thermohaline structure to the north. It is quite different from the Polar Front discontinuity, in that the higher surface salinity occurs to the south of the discontinuity rather than the north, and the *T*-min layer changes depth rather than terminates completely.

The Polar Front zone as shown in STD profiles extends from 56 to 62°S. The BT/XBT sections show the northern terminus of the *T*-min layer which marks the northern boundary of the Polar Front zone at 59°20'S on Figs. 8a–c, but the *T*-min is very broken between this latitude and 62°S.

The surface salinity at 59°20'S increases to over 34.0‰. Therefore, between 59°20'S and 62°20'S is a band of surface water below 34.0‰. This relatively fresh water is separated by nearly 300 km of saltier surface water from similar salinity surface water to the south, which, owing to its low temperature and proximity to the ice field, no doubt contains melt water. The northern belt of low salinity surface water results from the excess of precipitation over evaporation and perhaps from a contribution of melt water of previous years.

North of the Polar Front zone the water generally warms towards the north, with the pronounced cold water cell at 55°20'–56°20'S. Between these latitudes is also a zone with a low surface salinity. It is also shown by Sta. 1530 (Figs. 4 and 5) to

extend to great depths. The northern boundary of this feature is very intense, and is marked by a rapid surface-salinity increase; it is taken to be the Australasian sub-Antarctic front. The cold water of this feature suggests a divergent front, which may be the long-sought-after sub-Antarctic Divergence (IVANOV, 1959; WYRTKI, 1960; OSTAPOFF, 1962) to 'fit' between the Antarctic and subtropical convergences. An alternative model is given in Section 5 of this study which is based on advection from the southeast. The basic problem with an upwelling model is the occurrence of the low salinity at the surface (Fig. 8a) and upper 500 m (Sta. 1530), since in the case of upwelling higher surface salinity is expected.

The surface silicate traces in Figs. 8b and c indicate a sudden drop in silicate content of surface water on proceeding northward into the Polar Front zone at 62° to about 62°30'S. The decrease is from approximately 40  $\mu\text{g-atoms l}^{-1}$  first to near 10  $\mu\text{g-atoms l}^{-1}$  and then to less than 2  $\mu\text{g-atoms l}^{-1}$  at 61°15'–61°30'S. The surface silicate remains low to the north.

CLOWES (1938) shows the Antarctic Surface Water to have much higher silicate content in its southern range than in the northern part. Both sections, however, show large seasonal variation related to phytoplankton blooms, with the seasonal minimum occurring in October–November in the south and December–January in the northern parts of the Antarctic Surface Water. The *Eltanin* Cruise 50 data along 170°E were obtained at a time of minimum silicate in the northern parts and after the minimum in the southern. Clowes shows in his Fig. 9 that the rise in the south after the minimum is very rapid; hence the contrast between the two parts of the surface water increases throughout the summer months.

The source of the high surface silicate and salinity values is probably the upwelling deep water; it therefore is reasonable to conclude that the surface water south of 62°S contains more deep water and/or this deep water is not being diluted by fresher water nor is its silicate being consumed as rapidly as occurs to the north. The presence of the well-defined stratification of the *T*-min layer seems to preclude upwelling of CDW at the time of the Cruise 50 observations. Perhaps the high silicate concentration is a consequence of convective overturning down to the *T*-max layer initiated by winter period instability as discussed above.

##### 5. BAROCLINIC FIELD OF MASS

The meridional profile of specific volume anomaly, Fig. 9, shows the general downward slope of the isosteres is accomplished in three zones: over the continental slope, from the crest of the mid-ocean ridge to 58°S and just south of the Campbell Plateau escarpment. Reversals (slope down to the south) occur between 56 and 58°S, and to some extent south of the mid-ocean ridge, over the continental shelf over the Campbell Plateau. The specific volume anomaly is negative within the cold, saline shelf water mass of the Ross Sea. The *S*-max core layer approximates the 40  $\text{cl ton}^{-1}$  isostere north of the Polar Front, but crosses isosteres to the south, being less than 30  $\text{cl ton}^{-1}$  south of the mid-ocean ridge.

The slope of the isosteres gives an indication of the geostrophic flow direction and speed relative to the sea floor, i.e. the bottom referenced baroclinic velocity. In the southern hemisphere, a slope down to the north signifies an eastward current relative to the sea floor. The Cruise 50 segment of Fig. 9 is dealt with below; a few words may be said of the baroclinic current further south. The slope of the isosteres south of the

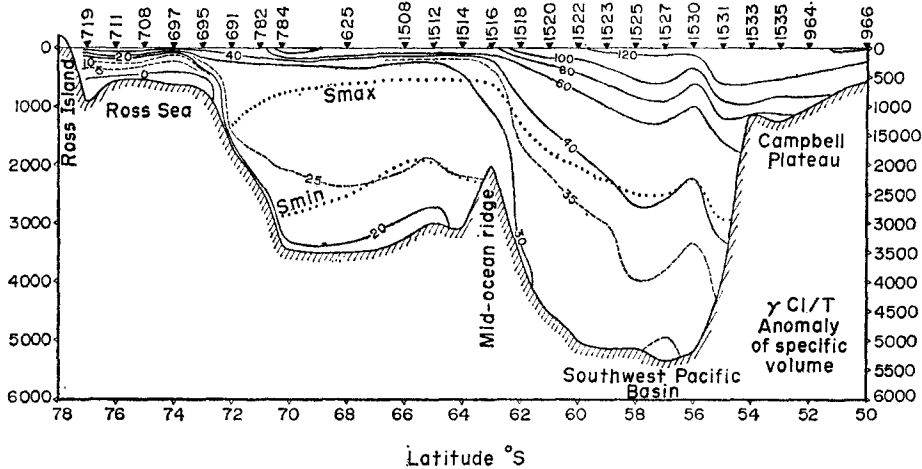


Fig. 9. Anomaly of specific volume on the 170°E meridional plane constructed from data of the stations shown in Fig. 1. The *S*-max and deep *S*-min core layer traces are shown.

mid-ocean ridge show a general weak baroclinic flow relative to the sea floor towards the west, with the pronounced exception of the continental slope region where an eastward, jet-like current is indicated. Observations from direct current measurements on the drift of ice-locked vessels (DEACON, 1937; SVERDRUP, 1953), and icebergs (TCHERNIA, 1974) consistently show westward motion over the outer continental shelf and slope, which is inconsistent with the bottom referenced baroclinic current. One suspects a significant barotropic component to velocity field, and/or a bottom zero reference layer is completely inappropriate for the continental margin. If the sea surface is used to determine the baroclinic velocity a strong westward flow at depth would be determined.

The baroclinic velocity field of the Cruise 50 data (Fig. 10a) shows strong flow over the northern flank of the mid-ocean ridge, between 58 and 60°S, and between 55 and 56°S, and a significant countercurrent (westward current) between 56 and 57°S. The southern high-velocity flow is the Antarctic Circumpolar Current, identified by its coincidence with the Polar Front zone, and the relation to the regional dynamic topography (GORDON and BYE, 1972). The northern eastward-flowing current is composed of warmer water and its origin is not clear, though some connection with the water passing through the deep gaps in the Macquarie Ridge is probable (BURLING, 1961; GORDON, 1972a; GORDON and BYE, 1972). The westward-directed current between 56 and 57°S suggests the presence of an intense cyclonic motion in this area which may feed the strong flow over the Campbell Plateau escarpment. This possibility is investigated with the aid of the *S*-max core layer depth (Fig. 7), which has been shown (GORDON, 1972a) to be a good approximation of the streamlines of geostrophic flow of the sea-surface relative to the 4000-dbar level.

The isobaths of the *S*-max layer indicate that the current, after passing the Macquarie Ridge in the fashion described in the introduction to this paper and by GORDON (1972a), undergoes a strong deflection to the south between 162 and 166°E, after which most flows eastward, mainly along 60°S, but a significant amount returns to give rise to the cyclonic motion associated with the feature shown by Sta. 1530 and in

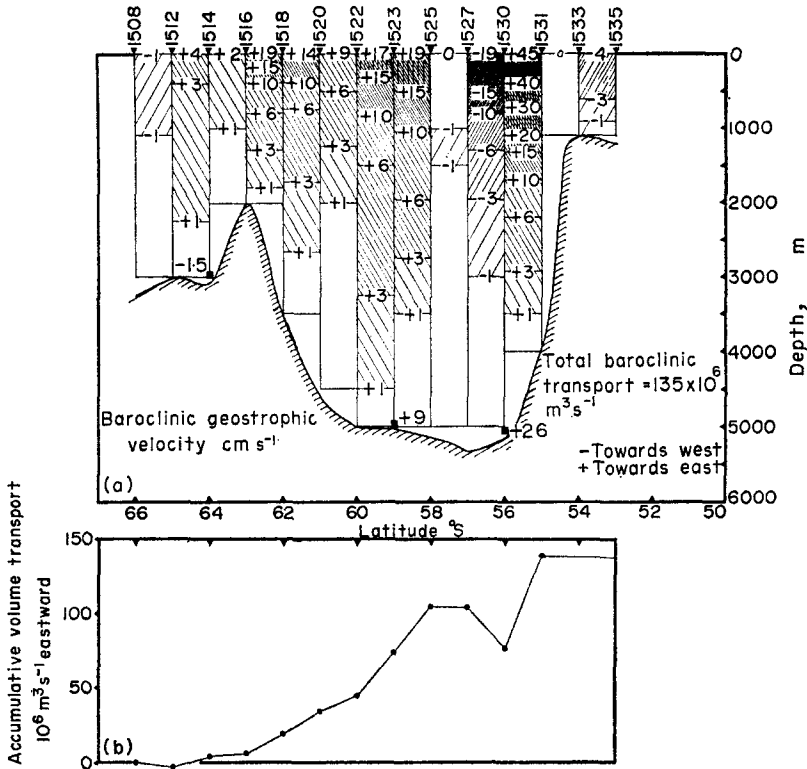


Fig. 10a. The geostrophic velocity between station pairs relative to their deepest common depth. b. The accumulative volume transport given by the velocity field relative to the deepest level, from 66°S northward.

the BT/XBT profile. This eddy may not be a steady-state feature, but rather a transient induced upstream.

The volume transport relative to the deepest common depth of station pairs is  $135 \times 10^6 \text{ m}^3 \text{ s}^{-1}$ , as compared to  $156 \times 10^6 \text{ m}^3 \text{ s}^{-1}$  and  $149 \times 10^6 \text{ m}^3 \text{ s}^{-1}$  calculated for 132°E and 115°E, respectively, by CALLAHAN (1971); the  $114 \times 10^6 \text{ m}^3 \text{ s}^{-1}$ , determined for the Drake Passage by REID and NOWLIN (1971) and  $165 \times 10^6 \text{ m}^3 \text{ s}^{-1}$  by KORT (1959).

The accumulated transport on proceeding northward from 66°S (Fig. 10b) shows the greatest rate of increase to be between 60 to 58°S and 56 to 55°S, with the leveling off and reduction plainly evident between 58 and 56°S. Since the bottom currents are not zero, this transport does not represent the absolute transport, but perhaps only 60–70% (GORDON, 1967; REID and NOWLIN, 1971; CALLAHAN, 1971).

Current meters were set out at 56, 59, and 64°S for slightly less than three days at the two northernmost positions and approximately 4 h at the southern position. The meters were placed 100 m above the sea floor. The results (Fig. 11) indicate significant bottom current, with major eastward components at 56 and 59°S and a northwest flow at 64°S. At 56°S the bottom current is exceptionally strong, averaging  $29 \text{ cm s}^{-1}$  towards 065° T (which is parallel to the Campbell Plateau escarpment). The eastward component averages  $26 \text{ cm s}^{-1}$  which considerably strengthens the eastward current

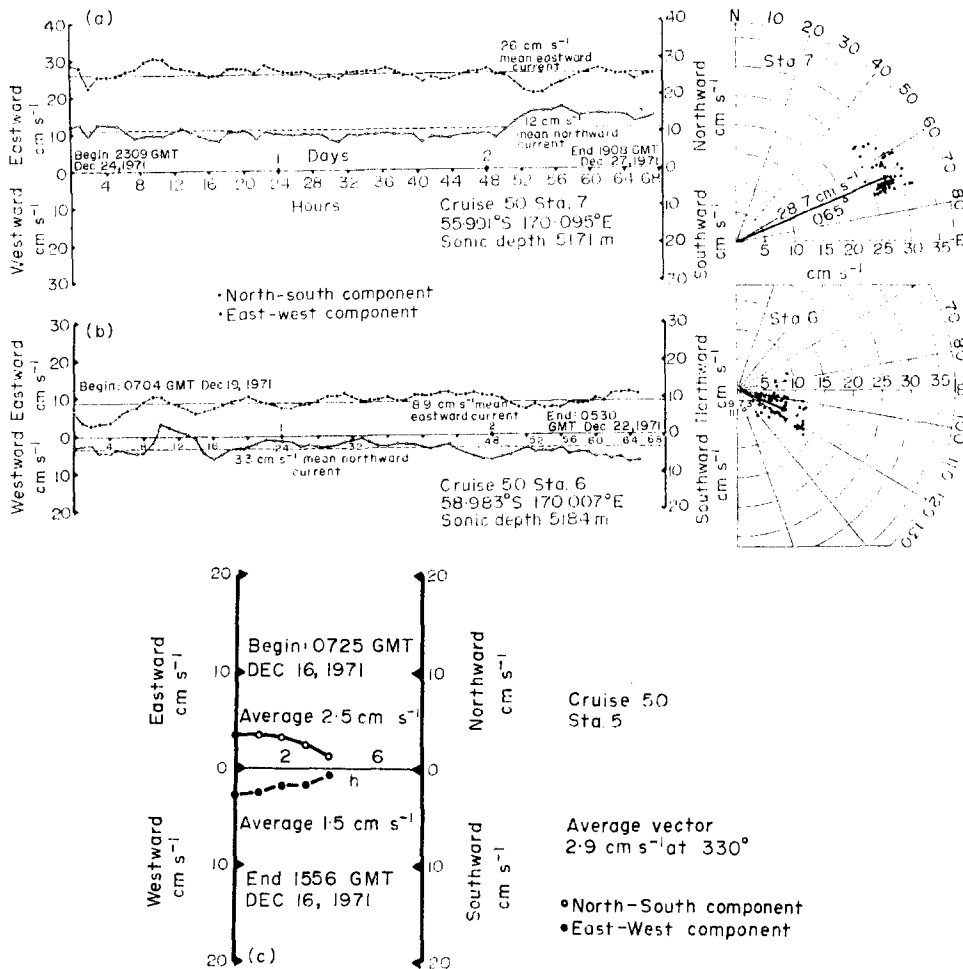


Fig. 11. Current-meter records of Cruise 50 along 170°E. Data given by plots of east-west and north-south components versus time, using hourly averaged data and using these same points on a polar coordinate plot. Data points were recorded approximately every minute. a. Station 7 at 56°S. b. Station 6 at 59°S. c. Station 5 at 64°S.

over the escarpment to nearly 1.5 knots and decreases the counterflow to minor speeds. It is apparent that the barotropic velocity field is not insignificant.

Compass-oriented bottom photographs at the 56°S station (Figs. 12 and 13) show an abundance of manganese nodules, which is taken as evidence of high bottom currents (HOLLISTER and HEEZEN, 1972). In Fig. 13 a non-stalked crinoid is observed on top of a boulder and is bent towards 070° T, which is down-current. It is possible that the crinoid (which is capable of motion) positioned itself on the rock so that the current will bend it into an eddy downcurrent of the boulder where food may be more concentrated (P. David, 1973, personal communication).

The short-period current measurement at 64°S shows a flow, along the trend of the ridges and valley, characteristic of the mid-ocean ridge (HAYES and CONOLLY, 1972). Though such a short-period record may not meaningfully reflect the 'climatic'

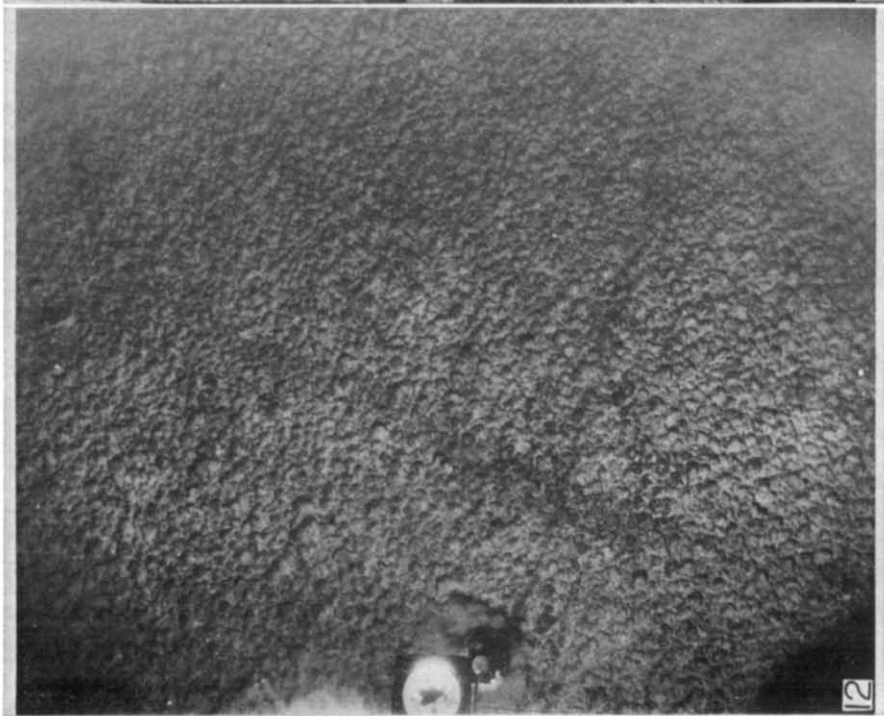


Fig. 12. Bottom photograph at  $55^{\circ}56'S$  and  $170^{\circ}01'E$ , frame 7 of camera Sta. 32, Cruise 50 of *Eltanin*. Magnetic declination correction to the compass which points towards the magnetic north is  $30^{\circ}E$ .



Fig. 13. Bottom photograph at  $55^{\circ}56'S$  and  $170^{\circ}01'E$ , frame 10 of camera Sta. 32, Cruise 50 of *Eltanin*. Same magnetic correction as Fig. 12 photograph.

bottom currents, it does indicate the possible escape of the saline AABW northward across the mid-ocean ridge via fracture zones.

## 6. CONCLUSIONS

(1) There are three regimes revealed by the thermohaline structure of the uppermost kilometer along 170°E from 53 to 66°S. The Polar Front zone from 56 to 62°S is relatively complex, with much interleaving of water types, which gives rise to structures with vertical scales of the order of 20–200 m. The northern limits of the multi-layered *T*-min occur just south of 59°S and are taken as an indication of the Polar Front or Antarctic Convergence. To the south of the Polar Front zone is the well-stratified Antarctic zone with horizontal isopleths and a continuous well-defined *T*-min layer near 100 m. Near 56°S (the northern boundary of the Polar Front zone) is a cell of cold, relatively low salinity water, which may be a transient feature associated with a strong cyclonic eddy. North of this feature the water column is more uniform and more typical of the Sub-Antarctic zone.

(2) The transitional layers between the deep water and the *T*-min layer of the surface water south of the Polar Front probably are maintained by a balance of upwelling to downward diffusion, in which case vertical mixing coefficients of 2–4 cm<sup>2</sup> s<sup>-1</sup> are determined.

(3) The *T/S* relation of the water column below the *S*-max core layer parallels the CDW/AABW baseline which results from mixing of warm, saline deep water which enters the Antarctic from the northern oceans, primarily the Atlantic, and the low-salinity variety of Antarctic Bottom Water with some influence of low salinity intermediate water in the Pacific Ocean. The point of departure of the *T/S* curve away from this baseline towards lower salinity marks the *S*-max core layer. North of the Polar Front this departure occurs at approximately 1.75°C. South of the Polar Front the *S*-max occurs at increasingly colder temperatures. It is concluded that south of the Polar Front the *S*-max results from the 'eroding' of the CDW/AABW baseline from above by the fresher, colder Antarctic layers. The *S*-max north and south of the front are, therefore, slightly different in nature: to the north it is a surface of spreading of the most saline of the deep waters, but to the south it is induced at lower salinity values as the deep water has a southward component of motion and is continuously being eroded from above by the differentially moving surface and transitional layers.

(4) The escape of the cold, saline shelf water of the Ross Sea is evident over the continental slope and deep ocean south of the mid-ocean ridge. This saline variety of bottom water causes a deviation of the *T/S* curves away from the CDW/AABW baseline towards higher salinity and induces a deep *S*-min south of the mid-ocean ridge.

(5) Surface salinity and silicates change abruptly at the discontinuity in the thermal structure near 62°S. South of this feature the salinity is 0.3‰ higher and silicates are 20-fold or more higher.

(6) The velocity field relative to the deepest common depth of station pairs indicates a bi-axial structure to the currents: a broad flow over the northern flank of the mid-ocean ridge and southern part of the Southwest Pacific Basin, and an intense, jet-like current over the Campbell Plateau escarpment. Between these currents is a counter-flow resulting from the action of a large, possibly transient, gyre south of the Campbell

Plateau, which returns some water northward after a southward shift between 162 and 165°E.

(7) Near-bottom current measurements at 56, 59, and 64°S indicate significant bottom currents, being over 0.5 knots at 56°S near the base of the Campbell Plateau.

*Acknowledgement*—The collection and processing of *Eltanin* Cruise 50 data was funded by GV 26230 of the National Science Foundation. The analysis of the data and the preparation of this paper was carried out while the author was on sabbatical leave from Columbia University in the City of New York. Much of the sabbatical leave was spent at 51°08'12''N and 0°38'54.1''W, the best known position (as of 2 January, 1970, by J. CREASE) of the Institute of Oceanographic Sciences, Wormley, England. The author is thankful to the IOS for providing a haven to carry out scientific research, Discussions with SIR GEORGE DEACON at IOS were of great aid to the author. The data processing was carried out at Lamont by S. S. JACOBS, T. ROOT, M. RODMAN and P. BRUCHHAUSEN.

#### REFERENCES

- BOLIN B. and H. STOMMEL (1961) On the abyssal circulation of the world ocean—IV. *Deep-Sea Research*, **8**, 95–110.
- BURLING R. W. (1961) Hydrology of circumpolar waters south of New Zealand. *Bulletin of the New Zealand Department of Scientific and Industrial Research*, **143**, 65 pp.
- CALLAHAN J. E. (1971) Velocity structure and flux of the Antarctic Circumpolar Current south of Australia. *Journal of Geophysical Research*, **76**(24), 5859–5870.
- CLOWES A. J. (1938) Phosphate and silicate in the Southern Oceans. *Discovery Reports*, **19**, 1–120.
- CRAIG, H., Y. CHUNG and M. FIADEIRO (1972) A benthic front in the South Pacific. *Earth and Planetary Science Letters*, **16**(1), 50–65.
- CRAIG, H. and L. I. GORDON (1965) Deuterium and oxygen 18 variations in the ocean and marine atmosphere. *Consiglio Nazionale Delle Ricerche*, 1–122.
- DEACON, G. E. R. (1933) A general account of the hydrology of the South Atlantic Ocean. *Discovery Reports*, **7**, 171–238.
- DEACON, G. E. R. (1937) The hydrology of the Southern Ocean. *Discovery Reports* **15**, 1–124.
- FOFONOFF, N. P. (1956) Some properties of sea water influencing the formation of Antarctic Bottom Water. *Deep-Sea Research*, **4**, 32–35.
- GERARD, R. D. and A. F. AMOS (1968) A surface-activated multiple sampler. *Marine Scientific Instruments*, **4**, 682–686.
- GILL A. E. (1973) Circulation and bottom water production in the Weddell Sea. *Deep-Sea Research*, **20**(2), 111–140.
- GORDON A. L. (1967) Structure of Antarctic waters between 20°W and 170°W. In: *Antarctic map folio series, folio 6*, V. BUSHNELL, editor, American Geographical Society, 10 pp.
- GORDON A. L. (1971a) Oceanography of Antarctic waters. In: *Antarctic oceanology I, Antarctic research series*, J. L. REID, editor, American Geophysical Union, Vol. 15, pp. 169–203.
- GORDON A. L. (1971b) Recent physical oceanographic studies of Antarctic waters. In: *Antarctic research*, L. QUAM and H. PORTER, editors, American Association for the Advancement of Science, pp. 609–629.
- GORDON A. L. (1971c) Antarctic polar front zone. In: *Antarctic oceanology I, Antarctic research series*, J. L. REID, editor, American Geophysical Union, pp. 205–221.
- GORDON A. L. (1972a) On the interaction of the Antarctic Circumpolar Current and the Macquarie Ridge. In: *Antarctic oceanology II, the Australian–New Zealand sector, Antarctic research series*, D. E. HAYES, editor, American Geophysical Union, Vol. 19, 71–78.
- GORDON A. L. (1972b) Spreading of Antarctic bottom water II. In: *Studies in physical oceanography—a tribute to George Wüst on his 80th birthday*, A. L. GORDON, editor, Gordon & Breach, Vol. 2, 1–17.
- GORDON A. L. (1973) Physical oceanography. *Antarctic Journal*, **8**(3), 61–68.
- GORDON A. L. and J. BYE (1972) Surface dynamic topography of Antarctic waters. *Journal of Geophysical Research*, **77**(30), 5993–5999.
- GORDON A. L. and R. D. GOLDBERG (1970) Circumpolar characteristics of Antarctic waters. In: *Antarctic map folio series, folio 13*, V. BUSHNELL, editor, American Geographical Society, pp. 1–15.
- GREGG M. C. and C. S. COX (1972) The vertical microstructure of temperature and salinity. *Deep-Sea Research*, **19**(5), 355–376.

- HAYES, D. E. and J. R. CONOLLY (1972) Morphology of the southeast Indian Ocean. In: *Antarctic oceanology II, the Australian–New Zealand sector, Antarctic research series*, D. E. HAYES, editor, American Geophysical Union, Vol. 19, pp. 125–145.
- HEEZEN, B. C., M. THARP and C. R. BENTLEY (1972) Morphology of the Earth in the Antarctic and Subantarctic. *Antarctic map folio series*, no. 16, American Geographical Society.
- HOLLISTER, C. D. and B. C. HEEZEN (1972) Geologic effects of ocean currents: western North Atlantic. In: *Studies in physical oceanography—a tribute to George Wüst on his 80th birthday*, A. L. GORDON, editor, Gordon & Breach, Vol. 2, pp. 37–66.
- HOWARD, A. (1940) Hydrology, programme of work and record of observations. *Report. B.A.N.Z. Antarctic Research Expedition 1921–31, Series A, Vol. 3, Oceanography, Part 2, Section 2*, 24–86.
- IVANOV, YU. A. (1959) Location and seasonal variability of the frontal zones in the Antarctic. *Doklady Akademii nauk SSSR*, **129**(4), 777–780.
- JACOBS S. S. and A. F. AMOS (1967) Physical and chemical observations in the southern oceans. USNS *Eltanin reports*, Cruises 22–27, 1966–1967. Technical Report I-CU-1-67, Lamont-Doherty Geological Observatory of Columbia University, 287 pp.
- JACOBS S. S., P. M. BRUCHHAUSEN and E. B. BAUER (1970) Hydrographic stations, bottom photographs and current measurements, USNS *Eltanin reports*, Cruises 32–36, 1968. Lamont-Doherty Geological Observatory of Columbia University, 460 pp.
- JACOBS S. S., P. M. BRUCHHAUSEN, F. L. ROSSELOT, A. L. GORDON, A. F. AMOS and M. BELLARD (1972) Hydrographic stations, bottom photographs, current measurements, nephelometer profiles, USNS *Eltanin reports*, Cruises 37–39, 1969; 42–46, 1970. Technical Report TR-1-CU-1-71, Lamont-Doherty Geological Observatory of Columbia University, 490 pp.
- KORT V. G. (1959) New data on the transport of Antarctic waters. (In Russian.) In: *Informatsionnyi Byulleten' Sovetskoj antarkticheskoi ekspeditsii 1955–1958*, No. 9, 31–34. (English translation, *Soviet Antarctic Expedition Information Bulletin*, **1**, 358–361, Elsevier, Amsterdam, 1964.)
- LYNN R. J. and J. L. REID (1968) Characteristics and circulation of deep and abyssal waters. *Deep-Sea Research*, **15**, 577–598.
- MOSBY H. (1934) The waters of the Atlantic Antarctic Ocean. *Scientific Results of the Norwegian Antarctic Expedition 1927–1928*, **11**, 1–131.
- OSTAPOFF F. (1962) The salinity distribution at 200 meters and the Antarctic frontal zones. *Deutsche Hydrographische Zeitschrift* **15**(4), 113–142.
- PINGREE R. D. (1972) Mixing in the deep stratified ocean. *Deep-Sea Research*, **19**(8), 549–562.
- REID J. L., JR (1965) Intermediate waters of the Pacific Ocean. *Johns Hopkins Oceanographic Studies* **2**, 85 pp.
- REID J. L. and R. J. LYNN (1971) On the influence of the Norwegian–Greenland and Weddell seas upon the bottom waters of the Indian and Pacific oceans. *Deep-Sea Research*, **18**, 1063–1088.
- REID J. L. and W. D. NOWLIN (1971) Transport of water through the Drake Passage. *Deep-Sea Research*, **18**, 51–64.
- STOMMEL H. and K. N. FEDOROV (1967) Small scale structures in temperature and salinity near Timor and Mindanao. *Tellus*, **19**(2), 307–325.
- SVERDRUP, H. U. (1940) Hydrology, Section 2, discussion. *Report B.A.N.Z. Antarctic Research Expedition 1921–31, Series A., Vol. 3, Oceanography, Part 2, Section 2*, 88–126.
- SVERDRUP H. U. (1953) The currents off the coast of Queen Maud Land. *Norsk geografisk tidsskrift*, **14**, 239–249.
- TCHERNIA P. (1974) Etude de la dérive antarctique Est–Ouest au moyen d'icebergs suivis par le satellite Eole. *Compte rendu hebdomadaire des séances de l'Académie des Sciences, Paris*, **278**, B, 667–670.
- THORNDIKE E. M. (1959) Deep-sea cameras of the Lamont Observatory. *Deep-Sea Research*, **7**(1), 10–16.
- WÜST, G. (1935) Schichtung und Zirkulation des Atlantischen Ozeans. *Wissenschaftliche Ergebnisse der Deutschen Atlantischen Expedition 'Meteor', 1925–27, Band VI, Teil 1, 2: Die Stratosphäre*.
- WRYTKI, K. (1960) The Antarctic Circumpolar Current and the Antarctic polar front. *Deutsche Hydrographische Zeitschrift*, **13**, 153–174.